Glycobiology, 2020, vol. 30, no. 7, 446–453
doi: 10.1093/glycob/cwz108
Advance Access Publication Date: 2 January 2020
Original Article

OXFORD

Cell Biology

The sialyltransferase ST6GAL1 protects against radiation-induced gastrointestinal damage

Patrick R Punch, Eric E Irons, Charles T Manhardt, Himangi Marathe†, and Joseph TY Lau[1]

Department of Molecular & Cellular Biology, Roswell Park Comprehensive Cancer Center, Elm & Carlton Streets, Buffalo, NY 14263, USA

[1]To whom correspondence should be addressed: Tel: (716) 845-8914; Fax: (716) 845-5908; e-mail: joseph.lau@roswellpark.org
†Present address: UB Clinical and Translational Science Institute, Jacobs School of Medicine and Biomedical Sciences, 955 Main Street, Buffalo, NY 14203, USA

Received 3 December 2019; Revised 19 December 2019; Editorial Decision 20 December 2019; Accepted 20 December 2019

Abstract

High-dose irradiation poses extreme risk of mortality from acute damage to the hematopoietic compartment and gastrointestinal tract. While bone marrow transplantation can reestablish the hematopoietic compartment, a more imminent risk of death is posed by gastrointestinal acute radiation syndrome (GI-ARS), for which there are no FDA-approved medical countermeasures. Although the mechanisms dictating the severity of GI-ARS remain incompletely understood, sialylation by ST6GAL1 has been shown to protect against radiation-induced apoptosis in vitro. Here, we used a C57BL/6 *St6gal1*-KO mouse model to investigate the contribution of ST6GAL1 to susceptibility to total body irradiation in vivo. Twelve gray total body ionizing γ-irradiation (TBI) followed by bone marrow transplant is not lethal to wild-type mice, but *St6gal1*-KO counterparts succumbed within 7 d. Both *St6gal1*-KO and wild-type animals exhibited damage to the GI epithelium, diarrhea and weight loss, but these symptoms became progressively more severe in the *St6gal1*-KO animals while wild-type counterparts showed signs of recovery by 120 h after TBI. Increased apoptosis in the GI tracts of *St6gal1*-KO mice and the absence of regenerative crypts were also observed. Together, these observations highlight an important role for ST6GAL1 in protection and recovery from GI-ARS in vivo.

Key words: gastrointestinal acute radiation syndrome, intestine, radiation biology, sialyltransferase, ST6GAL1

Introduction

Acute radiation exposure, whether accidental or malicious, poses significant risk of mortality due to extensive damage to the hematopoietic or gastrointestinal organ systems (Williams and McBride 2011; Castle et al. 2018). Radiation therapy delivered in close proximity to the gastrointestinal tract is often accompanied by both acute and chronic complications in the digestive system, resulting in significant morbidity (Yu 2013; Hauer-Jensen et al. 2014). In 2015, the use of granulocyte colony stimulating factor, or filgrastim in combination with bone marrow transplantation, was approved by the FDA for use by patients recovering from myeloablative chemo or radiation therapy and has been secured for the national stockpile in case of radiation emergencies (Satyamitra et al. 2017). On the other hand, medical countermeasures intended for treating radiation-induced damage to the gastrointestinal tract have not yet been identified (Singh et al. 2015).

The gastrointestinal acute radiation syndrome (GI-ARS) manifests as denudation of the intestinal barrier, ultimately resulting in a dysfunctional, leaky epithelium incapable of nutrient absorption, electrolyte transport and compromised ability to function as a barrier to prevent infection (Booth et al. 2012). Radiation-induced

apoptosis of enterocytes plays a major part in depletion of proliferative stem cells in the epithelial crypts, but a secondary, inflammation-mediated reaction also contributes to GI-ARS-associated mortality (Kirsch et al. 2010; Leibowitz et al. 2011; Chen et al. 2014; Huang et al. 2016). Mouse models utilized in the study of GI-ARS evaluate disease severity by assessing weight loss, diarrhea, GI histological damage and inflammation leading up to death within 10 d of total body γ-irradiation (TBI). While these symptoms can be attributed to massive apoptosis of GI epithelial cells resulting in the degradation of functional, regenerative crypts, the mechanisms dictating the extent of damage and ability to recover remain incompletely understood (Castle et al. 2018).

The sialyltransferase ST6GAL1 mediates the attachment of terminal sialic acids in α2,6 linkages to lactosamine structures on proteins of the cell surface and extracellular milieu. Increases in α2,6-linked sialic acids and the cognate ST6GAL1 protein have long been linked to inflammatory conditions (Yasukawa et al. 2005), and ST6GAL1 deficiency in vivo leads to increased inflammatory cell production (Nasirikenari et al. 2006), granulocyte recruitment (Nasirikenari et al. 2010) and excessive inflammatory cytokine release in acute inflammation models (Nasirikenari et al. 2019). Reports using in vitro culture models have also implicated ST6GAL1 in delaying radiation-induced apoptosis (Lee et al. 2008, 2012; Lee, Lee et al. 2010), death receptor-mediated cell death (Swindall and Bellis 2011; Holdbrooks et al. 2018) and stem cell proliferation (Swindall et al. 2013; Schultz et al. 2016). However, ST6GAL1 in acute radiation exposure of the intact animal in vivo has yet to be evaluated.

Here, we report that *St6gal1*-KO mice, unable to express functional ST6GAL1 protein, are especially susceptible to ionizing radiation compared to wild-type counterparts. When exposed to 12 Gy TBI, wild-type mice were uniformly rescued by bone marrow transplant (BMT) while the treatment proved fatal to all *St6gal1*-KO counterparts within 1 week. The ST6GAL1 status of hematopoietic donor cells had no effect on this observation. In comparison with wild-type counterparts, *St6gal1*-KO mice exhibited increased weight loss, GI permeability and diarrhea. Lasting destruction of GI epithelial cells and architecture, pronounced intestinal cleaved caspase-3 and the absence of regenerative crypts were observed in *St6gal1*-KO but not in wild-type mice. Together, our observations have identified a novel role for ST6GAL1 in protecting against radiation-induced damage to the GI epithelium and in preventing death from GI-ARS.

Results

Increased radiation sensitivity in the absence of functional ST6GAL1

Three mouse strains, differing only in the ability to express functional ST6GAL1 protein, were examined for their sensitivity to TBI. The *St6gal1*-KO mouse, globally deficient in functional ST6GAL1 (Hennet et al. 1998), the *St6gal1*-dP1, deficient only in liver-derived circulatory ST6GAL1 (Appenheimer et al. 2003) and C57BL/6 wild-type mouse with normal ST6GAL1 expression were compared. To avoid complications of bone marrow failure, all irradiated animals received 4×10^6 total bone marrow cells from wild-type donor mice within 4 h after exposure to 12 Gy TBI. All the wild-type ($n = 15$) and *St6gal1*-dP1 ($n = 5$) recipients survived beyond 3 weeks. In striking contrast, none of the *St6gal1*-KO animals ($n = 15$) survived more than 7 d after radiation exposure (Figure 1A). *St6gal1*-KO mice lost significantly more weight leading up to death than the wild-type counterparts (Figure 1B).

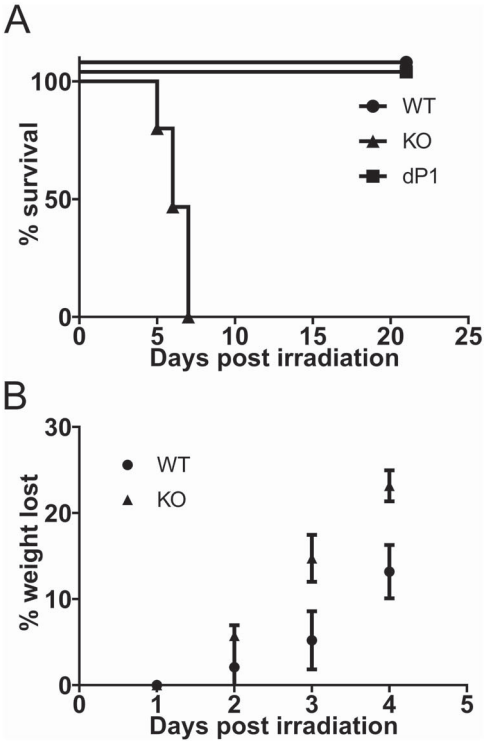

Fig. 1. ST6GAL1 deficiency results in increased sensitivity to TBI. (**A**) Wild-type C57Bl/6 (WT; $n = 15$), *St6gal1*-KO (KO; $n = 15$) and *St6gal1*-dP1 (dP1; $n = 5$) mice were subjected to 12 Gy TBI followed by intravenous infusion of 4×10^6 wild-type bone marrow cells. Morbidity was assessed as described in *Materials and methods*. All wild-type and *St6gal1*-dP1 animals survived beyond 3 weeks and none of the *St6gal1*-KO lived past 7 d [$P < 0.0001$ using Log Rank (Mantle-Cox) test]. (**B**) Body weight of wild-type (WT) and *St6gal1*-KO recipients in the initial 4 d post TBI ($n = 5$ KO and 5 WT recipients, with $^{**}P < 0.01$ and $^{***}P < 0.001$ for the weight difference between WT and KO on the indicated days).

ST6GAL1 regulates blood cell production at multiple levels, and absence of ST6GAL1 drives exaggerated neutrophilic and eosinophilic inflammation (Nasirikenari et al. 2006), which can be attenuated by elevating circulatory ST6GAL1 levels (Dougher et al. 2017). Therefore, we considered whether the ST6GAL1 status of transplanted marrow cells influences mortality in the irradiated animals. *St6gal1*-KO donor marrow cells, when transplanted into irradiated wild-type animals, did not render recipients susceptible to mortality (Figure 2A), indicating that TBI-induced mortality is not dependent on the ST6GAL1 status of the hematopoietic cells. This supplements our initial observation that *St6gal1*-KO animals could not be spared from death by transfusion of wild-type donor marrow cells (Figure 1A). Next, we considered the possibility that the ST6GAL1 status of irradiated recipients may influence homing and retention of transplanted cells in the bone marrow. Figure 2B and C shows that there is no difference in the ability of wild-type transplanted cells to migrate into (4 h) or to be retained in (120 h) the marrow of either genotype, respectively. Moreover, peripheral blood counts 120 h after TBI show similar circulating hematopoietic cell numbers, although peripheral cell counts are minimal, as expected for the time frame, in both recipient genotypes (Figure 2D). Histopathological analysis of the spleen, lung, kidneys and heart yielded no significant differences in damage or inflammation between the wild-type and *St6gal1*-KO recipients

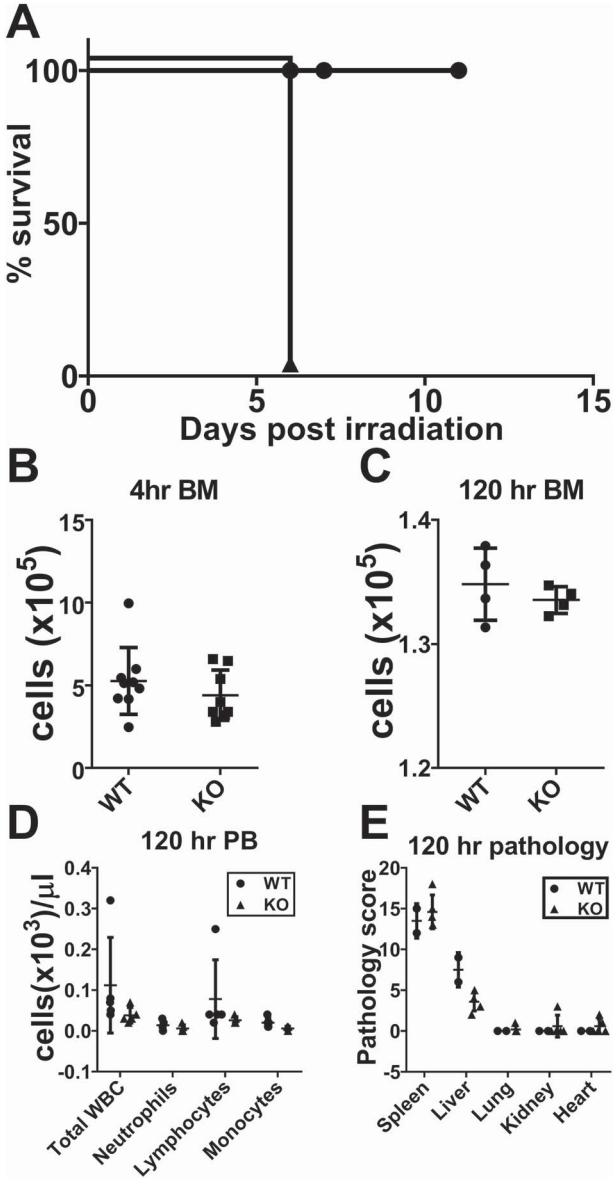

Fig. 2. Mortality of *St6gal1*-KO mice is not due to hematopoietic failure. (**A**) Wild-type or *St6gal1*-KO mice ($n = 6, 7$) were subjected to 12 Gy TBI followed by intravenous infusion of 4×10^6 *St6gal1*-KO bone marrow cells. (**B**, **C**) Similar homing and retention of transplanted wild-type marrow cells between recipient genotypes. Wild-type ($n = 9$) and *St6gal1*-KO ($n = 8$) mice were subjected to 12 Gy TBI followed by intravenous infusion of 4×10^6 wild-type bone marrow cells. Marrow harvested 4 and 120 h post procedure shows no difference between the recipient genotypes in homing and retention (4 and 120 h, respectively) of transplanted cells recovered in the recipient marrow. (**D**) Circulating blood counts in wild-type and St6gal1-ko recipients at day 5. There was minimal contribution of donor genotype hematopoietic cells to the peripheral circulating white cell pool 120 h post procedure in both wild-type and *St6gal1*-KO recipients. (**E**) Pathological evaluation, as described in *Materials and methods* and Supplemental Table SI, revealed no significant differences in organ damage between wild-type and *St6gal1*-KO recipients at 120 h in spleen, liver, lung, kidney and heart.

(Figure 2E). In the liver, there was mild-to-moderate radiation-associated damage that was slightly more severe in the wild-type than the *St6gal1*-KO mice (Figure 2E and Supplemental Table SI). This presentation was judged unlikely to be a factor driving death in the St6gal1-KO animals. Radiation-induced hepatic injury, though interesting, was not explored further here. These observations show that radiation-induced mortality in *St6gal1*-KO mice is not driven by an altered hematopoietic compartment or to multiorgan systems failure.

ST6GAL1 insufficiency increases susceptibility to TBI-induced GI damage

The timing of death and the lack of involvement of the hematopoietic compartment led to the hypothesis that the GI tract is likely playing a role in the mortality of *St6gal1*-KO mice. To assess damage to the GI tract, intestines from wild-type and *St6gal1*-KO animals at 24, 48, 72 and 120 h after TBI were subjected to histopathological evaluation. All irradiated recipients also received transplantation of wild-type marrow cells 4 h after TBI to minimize complications from marrow failure. Figure 3 summarizes the findings. Both genotypes exhibited slight increases in cellular infiltration within the lamina propria and submucosa 24 h after TBI (Figure 3A). GI damage and inflammation progressed similarly in both genotypes to 48 h, with both genotypes also exhibiting loss of epithelial cells. The degradation in architecture, denuding of villi and loss of crypt structures were more prominent in *St6gal1*-KO mice (Figure 3B). By 120 h, damage to epithelial architecture became even more striking in *St6gal1*-KO mice. Blunted and denuded villi, loss of crypts and increased inflammatory infiltration were prominent features of *St6gal1*-KO subjects. In contrast, signs of recovery were observed throughout the wild-type GI epithelium (Figure 3C). Nonirradiated wild-type and *St6gal1*-KO mice had no overt structural or cellular differences in villi length or crypt density (Supplemental Figure S1). The cell proliferation marker Ki67 was used to assess organ regeneration (Figure 3D, E, and F for 0, 24 and 120 h, respectively). Especially noteworthy is the widespread epithelial proliferation indicative of organ regeneration in the wild-type intestine, which was largely absent in the *St6gal1*-KO counterparts (Figure 3F).

Decreased GI function and increased apoptosis in the absence of functional ST6GAL1

In order to confirm the GI-ARS phenotype observed in *Stgal1*-KO mice, assessments of GI functionality were performed. Average length of villi was used as a metric to compare organ regeneration. At 120 h ST6GAL1 insufficiency resulted in 2.2-fold shorter average length of villi [166 ± 7 µm ($n = 47$)], compared to wild-type [369 ± 17 µm ($n = 30$)] (Figure 4A). The *ST6gal1*-KO gut also had strikingly reduced number of proliferative crypts compared to wild-type gut, as assessed by counting the number of crypts containing distinct $Ki67^+$ cells at 102 h (2.3 ± 0.67, $n = 3$ for *St6gal1*-KO compared to 15.3 ± 0.33, $n = 3$ for wild-type) (Figure 4B). Diarrhea was also more severe in *St6gal1*-KO mice based on the number of fully formed colonic fecal pellets 72 h after TBI, although statistical significance for the difference by this metric was not reached (Figure 4C). Assessment of GI permeability by the use of FITC-dextran assay revealed 1.7-fold higher serum fluorescence in ST6GAL1-deficient animals compared to wild-type (Figure 4F).

The presence of cleaved caspase-3, an indicator of apoptosis, was increased in GI cell lysates from *St6gal1*-KO mice 48 h after 12 Gy TBI compared to wild-type (Figure 4D). Treatment of *St6gal1*-KO irradiated mice with the necroptosis inhibitor necrostatin-1 failed to delay mortality, indicating that necroptotic cell death is not a major driver of *St6gal1*-KO mortality (Figure 4E). Professional pathologic evaluation of the GI tracts of wild-type ($n = 2$) and *St6gal1*-KO

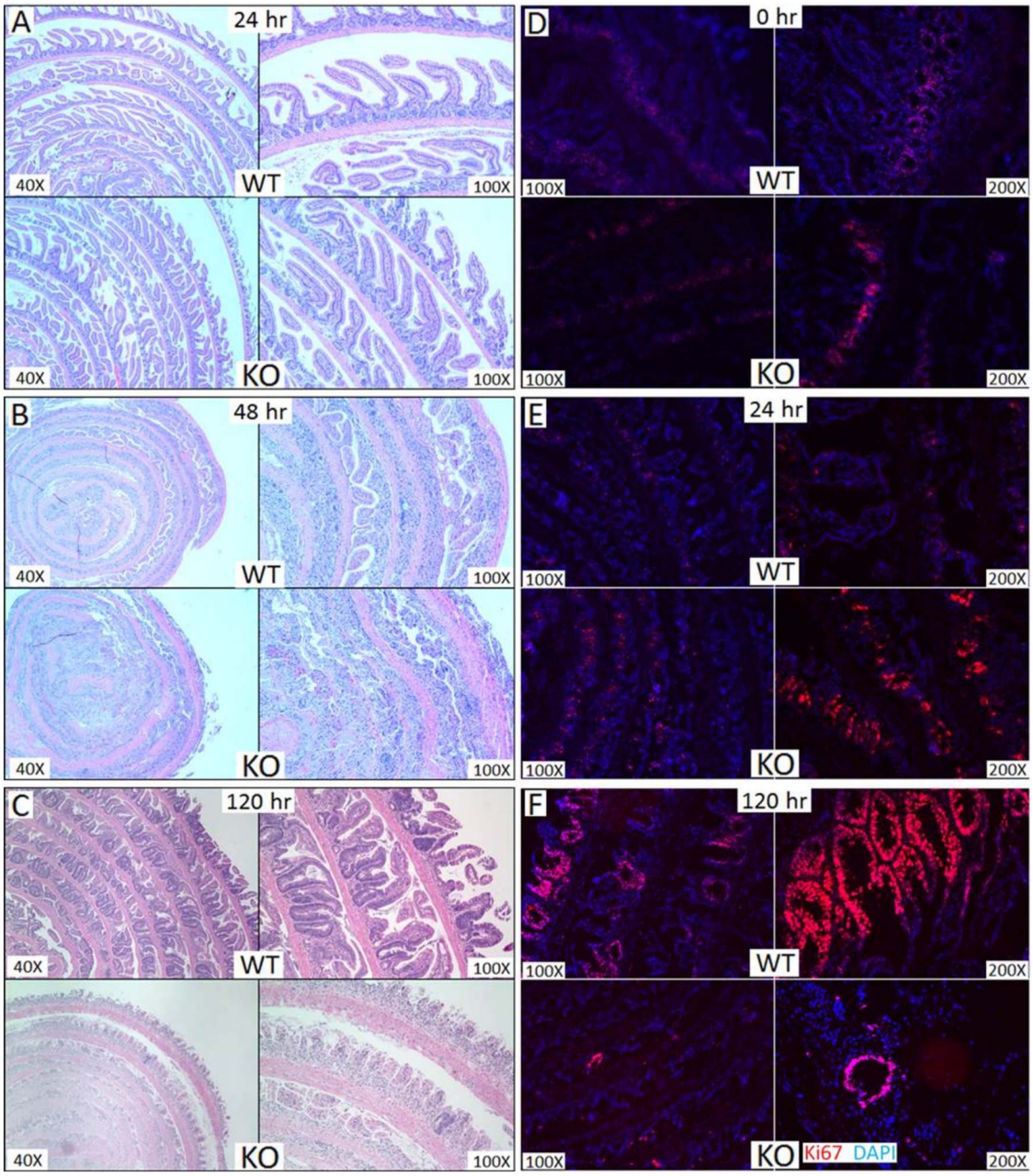

Fig. 3. *St6gal1*-KO recipients had more severe gastrointestinal damage than wild-type recipients. (**A**–**C**) Small intestines of recipients at 24, 48 and 120 h, respectively, after 12 Gy TBI followed by intravenous infusion of 4×10^6 wild-type bone marrow cells were evaluated by hematoxylin and eosin staining. Small intestine sections of wild-type and *ST6gal1*-KO mice were evaluated for Ki67 staining (red) at 0 h (**D**), 24 h (**E**) and at 120 h (**F**) post TBI and BMT as described in *Materials and methods*. This figure is available in black and white in print and in color at *Glycobiology* online.

($n = 5$) mice was performed 120 h after TBI. The findings are summarized in Figure 4G and Supplemental Table SII. The criteria used for evaluation are detailed in *Materials and methods*. In all tissues assessed, the most drastically increased pathologies in *St6gal1*-KO compared to wild-type were mucosal injury, inflammation and fibroplasia of the lamina propria. Cystic dilation of glands, only encountered in the colon, was also more severe in *St6gal1*-KO animals. These observations, taken together, demonstrate that *St6gal1*-KO animals are strikingly more susceptible to GI-ARS after 12 Gy TBI than wild-type counterparts.

Discussion

ST6GAL1 was among the first glycosyltransferases characterized and purified in the 1980s (Weinstein et al. 1987; Svensson et al. 1990) and was intensely studied in the 1990s due to its association with the acute phase response (Jamieson et al. 1993) and dysregulation in several malignancies (Dall'Olio et al. 1989; Petretti et al. 1999; Wang et al. 2003; Wichert et al. 2018). Since that time, interest in the enzyme has waned due to the lack of concrete and in depth understanding of the physiologic role of the sialyltransferase and its catalytic product, the α2,6-linked sialic acids found on *N*-glycans.

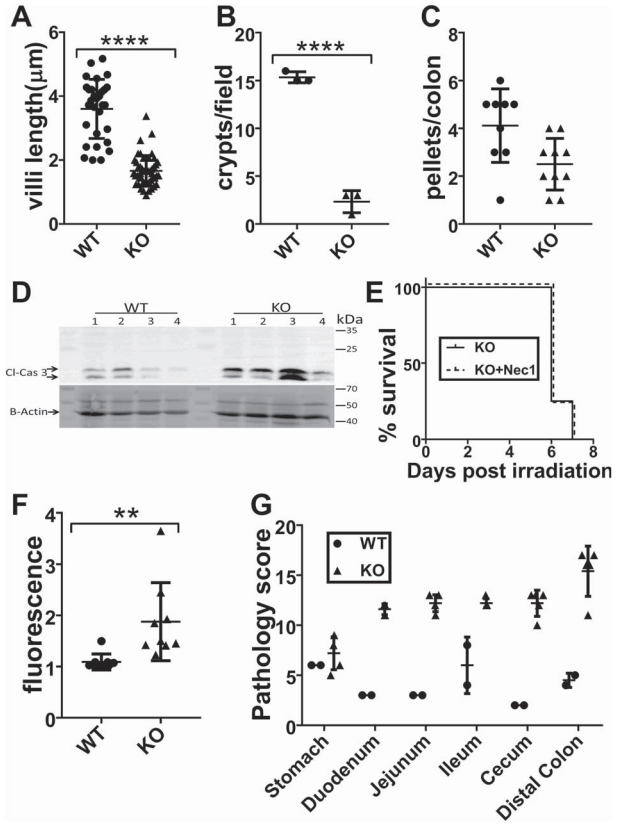

Fig. 4. Increased cell death and decreased GI function in *ST6gal1*-KO animals. (**A**) Intestinal villi length was measured from four fields of view from three different animals per genotype ($n = 30$ WT, $n = 47$ KO) 120 h after TBI. Average length of WT villus (369 ± 17 μm) was >2-fold longer than the average KO villus (166 ± 7 μm) ($P < 0.0001$). (**B**) 120 h after TBI the number of proliferative crypts per field of view was higher in WT (15.3 ± 0.33, $n = 3$), compared to KO (2.33 ± 0.67, $n = 3$) ($P < 0.0001$). (**C**) Diarrhea was quantified by counting the number of fully formed fecal pellets in colons of irradiated mice at 72 h after TBI and BMT. (**D**) Increased cleaved caspase 3 in the GI tracts of *St6gal1*-KO mice compared to wild-type 48 h after 12 Gy TBI and BMT. (**E**) *ST6gal1*-KO mice were treated with necrostatin-1, an inhibitor of necroptosis 24 h after TBI (from Chen et al. 2014). This treatment (which delayed death in a previous study) did not delay mortality of *St6gal1*-KO mice. ($N = 5$). (**F**) Oral gavage of FITC-dextran was administered at 120 h after TBI and BMT, showing greater levels of FITC-dextran leakage into the blood of *St6gal1*-KO animals. (**G**) Summary of pathological scoring indicating that at 120 h after TBI and BMT, *St6gal1*-KO mice had significantly more gastrointestinal damage than wild-type mice in all portions of the GI tract assessed except for the stomach. Evaluation criteria are given in Supplemental Table SII.

A resurgence of recent interest has been stimulated by mechanistic reports of the role of ST6GAL1 in modifying several key signaling pathways. In particular, reports have linked ST6GAL1 upregulation with increased chemo- (Schultz et al. 2016; Britain et al. 2018; Chakraborty et al. 2018) and radio-resistance (Lee et al. 2008, 2012; Lee, Park et al. 2010). However, these observations were made in cultured cell lines in vitro. Here, we extend upon these observations by assessing the participation of ST6GAL1 in radio-resistance in vivo. We observed that mice without functional ST6GAL1 are exquisitely more sensitive to high-dose total body ionizing radiation than their wild-type counterparts. Mortality from high-dose TBI is generally a result of destruction of the hematopoietic compartment or the gastrointestinal tract, or both. Because medical countermeasures for the hematopoietic acute radiation syndrome (H-ARS) already exist, we chose to expose mice to a dose of 12 Gy, likely to confer significant but repairable damage to the gastrointestinal tract of wild-type C57BL/6 mice, followed by bone marrow transplantation to protect the hematopoietic compartment. The regimen used and the timing of death of *St6gal1*-KO mice strongly suggested that mortality was due to GI-ARS rather than H-ARS. Similar hematopoietic recovery and the fact that the ST6GAL1 status of bone marrow donor cells did not alter the mortality of *St6gal1*-KO nor wild-type irradiated mice further suggest that this phenotype is primarily not due to hematopoietic failure.

At day 5 post TBI, there was no difference in observed pathology to other critical organs between wild-type and *St6gal1*-KO animals, including spleen, liver, lung, kidney and heart. Differences in the gastrointestinal system were therefore further implicated. Increased mortality was accompanied by symptoms indicative of GI-ARS including increased weight loss and more severe diarrhea and GI permeability. We also observed a striking lack of proliferative epithelial cells working to regenerate a functional GI epithelium. While the mechanisms driving the onset and severity of GI-ARS remain poorly understood, the inflammation-driven mucositis as well as a number of cell death pathways are implicated, including p53-mediated apoptosis and death receptor-mediated necroptosis (Qiu et al. 2008; Leibowitz et al. 2011; Booth et al. 2012; Chen et al. 2014; Stoecklein et al. 2015; Huang et al. 2016). Indeed, we observed increased cleaved caspase-3 in the GI of ST6GAL1-deficient animals 3 d post TBI.

There is a conundrum of a profound gastrointestinal phenotype associated with ST6GAL1 deficiency, when *St6gal1* is in general transcriptionally silent in the small intestines of adult mice. ST6GAL1 expression and its cognate α2,6-linked sialic acid are restricted to the distal colon of adults (Dai et al. 2002). Studies using human tissue samples indicate that ST6GAL1 expression in the GI tract is limited to a small number of cells occupying crypt structures and that this expression may maintain stem cells in a quiescent state; however, this has not been observed in the mouse. Inability to express ST6GAL1 may render crypt stem cells susceptible to radiation-induced cell death, thus compromising the regenerative ability of the intestinal epithelium. In support of this mechanism driving mortality of ST6GAL1-deficient mice, we observed signs of restoration of the epithelium by day 5 in the wild-type but not in the *St6gal1*-KO intestine, including extensive Ki67 incorporation in proliferating cells of the wild-type but not *St6gal1*-KO gut (Figure 3D).

Taken together, our data show a role for functional ST6GAL1 and the cognate α2,6 sialylated *N*-linked glycans in protection against ionizing radiation in vivo using mouse models. While radiation damages the gut regardless of ST6GAL1 status, the protection afforded by the presence of the sialyltransferase pertains to preserving the regenerative ability of the gut epithelium, which normally needs to renew itself once every 72 h (Leedham et al. 2005; Barker et al. 2007). While remaining to be demonstrated directly, the current data suggest the ability of functional ST6GAL1 to protect the intestinal stem cells needed for epithelial regeneration from radiation damage. Indeed, in cultured cells, the presence of ST6GAL1 contributes to tumor spheroid growth of ovarian cancer cells and increases the chemoresistance of ovarian cancer cells to gefitinib (Schultz et al. 2016; Britain et al. 2018) and the resistance of pancreatic cancer cell lines to gemcitabine (Chakraborty et al. 2018). Moreover, ST6GAL1 has been implicated in conferring "stemness" to cancer cell lines and in preventing radiation-induced apoptosis of colon cancer cell lines. While further studies will be needed to determine the precise mechanistic role of ST6GAL1 in radiation-induced death in gastrointestinal

damage, manipulating ST6GAL1 and sialylation status may provide a novel therapeutic modality. On the one hand, increasing ST6GAL1 activity may confer protection against unintentional radiation damage; alternatively, decreasing the activity may increase the efficacy of current chemotherapies and radiation regimens in the treatment of malignant diseases.

Materials and methods

Animals, irradiation and bone marrow transplantation

The experimental protocols were reviewed and approved by the Institutional Animal Care and Use Committee (IACUC) and Roswell Park Comprehensive Cancer Center (RPCCC). Age (8–12 weeks) and sex-matched WT C57BL/6, *St6gal1*-dP1-C57Bl/6 or *St6gal1*-KO C57Bl/6 mice were exposed to a single 12 Gy dose of ionizing radiation from a Shephard Mark-I irradiator, model 68, 4000 Ci Cesium 137 source irradiator (J.L. Shepherd and Associates). Mice were held in a pie-shaped container on a rotating turntable without anesthesia during irradiation. Up to eight mice were irradiated at once. The average dose rate was 1.04–1.1 Gy/min. In cases requiring subsequent bone marrow transplantation, irradiated mice were injected via tail vein with 4×10^6 whole bone marrow cells from either WT B6 45.1 (Pep Boy), WT C57Bl/6 or *St6gal1*-KO C57Bl/6 mice within 4 h of TBI. Briefly, donor mice were euthanized and bone marrow cells collected from femurs and tibia by flushing with DPBS. Bones were then crushed, rinsed in PBS, briefly vortexed and supernatant was collected to maximize cell yield. After red blood cell lysis, cells were centrifuged at 1200 rpm for 8 min at 4°C and resuspended in sterile PBS to a concentration of 2×10^7 cells/mL, and 200 µL of this cell solution was injected via tail vein.

Mouse monitoring and gross pathology

Irradiated mice were monitored twice daily for signs of morbidity including response to touch, lethargy, hunching and ruffling of fur. Mice were euthanized upon observation of severe lethargy and lack of response to touch. Mice were also monitored for weight loss once daily and were sacrificed when total weight lost exceeded 30% of starting weight.

Briefly, the criteria used in creating the overall pathology scores for each tissue section are defined as follows: (1) mucosal injury, including apoptosis, necroptosis, sloughing of cells or loss of normal mucosal architecture; (2) cystic dilation of glands; (3) mucosal hyperplasia characterized by any type of proliferative changes prevalent in GI mucosa; (4) inflammation or the presence of inflammatory cell infiltrates and (5) fibroplasia of the lamina propria.

Tissue acquisition

Mice were euthanized and intestines were isolated for protein analysis or histology at various time points indicated below. Mice were asphyxiated with CO_2 followed by cervical dislocation. Intestines were excised beginning approximately 1 cm distal to the stomach to approximately 1 cm proximal to rectum. Small intestines were then divided into three sections roughly corresponding to the duodenum, jejunum and ileum; the cecum was removed and the colon isolated. Solid fecal matter was gently removed and intestine sections were flushed with PBS using a syringe and blunt end needle. Tissue samples were then further processed for protein analysis of histology as described below.

Preparation of intestinal tissue homogenates

Intestinal tissue homogenates for protein analysis at various time points were prepared as follows. Intestines from WT and KO mice were harvested 72 h postirradiation, snap frozen and stored at −80°C until homogenized. Tissues were crushed with a mortar and pestle in liquid nitrogen until powder was formed and then incubated with cell lysis buffer (50 mM Tris, pH 6.8, 2% SDS, 10% glycerol with protease inhibitor (complete mini from (Sigma, # 11836170001: 1 tablet/10 mL)) and 40 mM sodium orthovanadate being added directly prior to use) on ice for 20 min. Samples were then sonicated briefly and centrifuged at 10,000 rpm for 10 min at 4°C, supernatant was removed and samples were stored at −80°C until further use.

Western blot

Intestinal tissue homogenates were used for western blot analysis of caspase-3 activation. Protein concentration of prepared homogenates was determined using Pierce BCA protein assay kit (Thermo Fisher #23225). Protein samples were denatured at 95°C for 5 min in Laemmli buffer. About 10 µg protein was loaded per well into a 12% SDS polyacrylamide gel, subjected to electrophoresis and transferred onto a PDVF membrane. Membrane was rinsed briefly with TBST, blocked with Protein-Free T20 (TBS) Blocking Buffer (Thermo Fisher #37571) for 1 h at room temperature and then incubated overnight at 4°C with primary antibody to cleaved caspase-3 (Asp175; Cell Signaling Technologies #9661) diluted 1:1000 in blocking buffer. Membrane was washed twice with TBST quickly and then incubated for 1 h at room temperature with secondary antibody HRP-conjugated Goat anti-rabbit IgG (Invitrogen, #A16096) diluted 1:5000 in TBST. Membrane was developed using Pierce ECL Western Blotting Substrate (Thermofisher #32106) and imaged on Biorad Chemidoc Touch. Membrane was then rinsed, reblocked and reprobed using antibody to beta-actin (clone BA3R; Invitrogen #MA5-15739) diluted 1:2000 as a loading control, with secondary antibody HRP-conjugated goat anti-mouse IgG (H/L): HRP (BioRad #STAR207P) diluted 1:5000 in TBST. Membrane was then developed with ECL and imaged as before.

Histology and immunofluorescence

Intestines were isolated and cleaned as described (see tissue acquisition) and then further processed for histological examination. In the case of "Swiss rolled" small intestine or colons, sections were opened laterally, rinsed with DPBS, rolled around a toothpick with intestinal lumen facing outward and stored in 10% formalin until sectioning. In the case of frozen sections, intestines were Swiss-rolled and then snap-frozen in liquid nitrogen until sectioning. All Swiss-rolls begin with the most proximal portion of the tissue in the center of the roll and the most distal in the outer layer. In some instances, Swiss-rolling was not performed. In these cases, intestines and colons were isolated and flushed with PBS as described and then flushed with 10% formalin before being placed in 10% formalin until sectioning. Tissue sectioning, slide preparation and hematoxylin and eosin staining were performed at the Roswell Park Comprehensive Cancer Center Histology Core Facility. In all instances, samples were sectioned at 5 µm thickness. About 5 µm frozen section slides prepared by RPCCC Histology Core Facility were used for immunofluorescent detection of proteins in Figure 3.

For cleaved caspase-3 immunofluorescence, 5 µm frozen sections were placed in ice-cold acetone for 10 min, rinsed with DPBS and incubated with blocking solution (10% FBS in DPBS) for 1 h at

room temperature. Slides were then washed with DPBS 3× for 5 min each before primary antibody incubation (all 14–18 h at 4°C) as follows: cleaved caspase-3 (Asp175; Cell Signaling Technologies #9661) diluted 1:400 in blocking solution; Ki67 (clone SP6; Invitrogen # MA5-14520) diluted 1:250. After primary antibody incubation, slides were washed 3× with DPBS for 5 min each and then incubated with secondary antibody (DyLight 549 Affinipure Goat Anti Rabbit IgG; Jackson #111-505-003), stored in 50% glycerol and diluted 1:500 in blocking solution. All slides were then washed 2× with DPBS for 3 min each, stained with DAPI (2.2 µM) diluted in DPBS for 5 min, washed with DPBS and finally coverslips were applied using VectaShield Antifade Mounting Medium (Vector labs #H-1000).

Quantification of crypt density and villi length

Villi length and crypt density 120 h post irradiation were measured using full size, undoctored histological images. Villi length was quantified from four fields of view from three different animals per genotype. Crypt density, measured as number of intact crypts containing at least one distinct $Ki67^+$ cell per field of view, was quantified from three images per genotype, each from a separate mouse.

Microscopy

All histological images were obtained using a Nikon Eclipse (Model # E600, Japan) microscope and a SPOT RT3 (Model # 25.42Mp Slider) camera with SPOT 5.2.7 software (Build 15550). Uncropped and undoctored images were used in all figures.

FITC-dextran assay for GI permeability

FITC-dextran (FD4) was purchased from Sigma-Aldrich. WT and *Stgal1*-KO mice, either receiving neither TBI nor BMT or undergoing 12 Gy TBI and BMT, were fasted for 4 h beginning 5 d after TBI. FITC-dextran was administered (100 µL, 2.5 mg) via oral gavage, followed by 3 h fasting. Blood was collected via retro-orbital bleeding, mice were euthanized and serum samples were prepared. Serum was diluted and fluorescence was measured by Synergy HTX microplate reader with excitation at 490 nm and emission at 520 nm.

Necrostatin-1 treatment

Necrostatin-1 (Tocris, #2324), dissolved in sterile DMSO to concentration of 30 mM then diluted (8.5 µL/mL) in sterile DPBS, was injected intraperitoneally (500 µL, 33 µg per mouse) approximately 24 h post-12 Gy TBI with BMT (as previously described), according to (Chen et al. 2014). DMSO diluted in sterile DPBS (8.5 µL/mL DPBS) was used as negative control.

Author contributions

P.R.P. conceived, designed and performed experiments and wrote manuscript. E.E.I., C.T.M. and H.M. contributed to design and execution of experiments. J.T.Y.L. provided critical oversight, conceived and designed research and wrote the manuscript.

Supplementary data

Supplementary data for this article is available online at http://glycob.oxfordjournals.org/.

Funding

National Institute of Allergy and Infections Diseases (R01AI140736). The core facilities of Roswell Park Comprehensive Cancer Center used in this work were supported in part by National Institutes of Health National Cancer Institute Cancer Center Support (CA076056). Cytometry services were provided by the Flow and Image Cytometry Core facility at the Roswell Park Comprehensive Cancer Center, which is supported in part by the National Cancer Institute Cancer Center Support (5P30 CA016056).

Conflict of interest

None declared.

Acknowledgements

The expert technical assistance of Valerie Andersen, M.S., is greatly acknowledged.

Abbreviations

BMT, bone marrow transplant; DAPI, 4′,6-diamidino-2-phenylindole; DPBS, Dulbecco's phosphate buffered saline; GI-ARS, gastrointestinal acute radiation syndrome; H-ARS, hematopoietic acute radiation syndrome; PDVF, polyvinylidene fluoride; TBI, total body ionizing irradiation.

References

Appenheimer MM, Huang R-Y, Chandrasekaran EV, Dalziel M, Hu YP, Soloway PD, Wuensch SA, Matta KL, Lau JTY. 2003. Biologic contribution of P1 promoter-mediated expression of ST6Gal I sialyltransferase. *Glycobiology*. 13(8):591–600.

Barker N, Van Es JH, Kuipers J, Kujala P, Van Den Born M, Cozijnsen M, Haegebarth A, Korving J, Begthel H, Peters PJ. 2007. Identification of stem cells in small intestine and colon by marker gene Lgr5. *Nature*. 449(7165):1003.

Booth C, Tudor G, Tudor J, Katz BP, MacVittie TJ. 2012. Acute gastrointestinal syndrome in high-dose irradiated mice. *Health Phys*. 103(4):383–399.

Britain CM, Holdbrooks AT, Anderson JC, Willey CD, Bellis SL. 2018. Sialylation of EGFR by the ST6Gal-I sialyltransferase promotes EGFR activation and resistance to gefitinib-mediated cell death. *J Ovarian Res*. 11(1):12.

Castle KD, Daniel AR, Moding EJ, Luo L, Lee C-L, Kirsch DG. 2018. Mice lacking RIP3 kinase are not protected from acute radiation syndrome. *Radiat Res*. 189(6):627–633.

Chakraborty A, Dorsett KA, Trummell HQ, Yang ES, Oliver PG, Bonner JA, Buchsbaum DJ, Bellis SL. 2018. ST6Gal-I sialyltransferase promotes chemoresistance in pancreatic ductal adenocarcinoma by abrogating gemcitabine-mediated DNA damage. *J Biol Chem*. 293(3):984–994.

Chen Q, Xia X, Wu S, Wu A, Qi D, Liu W, Cui F, Jiao Y, Zhu W, Gu Y *et al.* 2014. Apoptosis, necrosis, and autophagy in mouse intestinal damage after 15-Gy whole body irradiation. *Cell Biochem Funct*. 32(8):647–656.

Dai D, Nanthakumar NN, Savidge TC, Newburg DS, and Walker WA. 2002. Region-specific ontogeny of alpha-2,6-sialyltransferase during normal and cortisone-induced maturation in mouse intestine. *American journal of physiology. Gastrointestinal and liver physiology*. 282, G480–490.

Dall'Olio F, Malagolini N, di Stefano G, Minni F, Marrano D, Serafini-Cessi F. 1989. Increased CMP-NeuAc:Gal beta 1,4GlcNAc-R alpha 2,6 sialyltransferase activity in human colorectal cancer tissues. *Int J Cancer*. 44(3):434–439.

Dougher CWL, Buffone A, Nemeth MJ, Nasirikenari M, Irons EE, Bogner PN, and Lau JTY. 2017. The blood-borne sialyltransferase ST6Gal-1 is

a negative systemic regulator of granulopoiesis. *Journal of Leukocyte Biology*. 102, 507–516.

Hauer-Jensen M, Denham JW, Andreyev HJN. 2014. Radiation enteropathy—Pathogenesis, treatment and prevention. *Nat Rev Gastroenterol Hepatol*. 11(8):470–479.

Hennet T, Chui D, Paulson JC, Marth JD. 1998. Immune regulation by the ST6Gal sialyltransferase. *Proc Natl Acad Sci USA*. 95(8):4504–4509.

Holdbrooks AT, Britain CM, Bellis SL. 2018. ST6Gal-I sialyltransferase promotes tumor necrosis factor (TNF)-mediated cancer cell survival via sialylation of the TNF receptor 1 (TNFR1) death receptor. *J Biol Chem*. 293(5):1610–1622.

Huang Z, Epperly M, Watkins SC, Greenberger JS, Kagan VE, Bayır H. 2016. Necrostatin-1 rescues mice from lethal irradiation. *Biochim Biophys Acta*. 1862(4):850–856.

Jamieson JC, McCaffrey G, Harder PG. 1993. Sialyltransferase: A novel acute-phase reactant. *Comp Biochem Physiol B Comp Biochem*. 105(1): 29–33.

Kirsch DG, Santiago PM, di Tomaso E, Sullivan JM, Hou W-S, Dayton T, Jeffords LB, Sodha P, Mercer KL, Cohen R *et al*. 2010. p53 controls radiation-induced gastrointestinal syndrome in mice independent of apoptosis. *Science (New York, NY)*. 327(5965):593–596.

Lee M, Lee H-J, Bae S, Lee Y-S. 2008. Protein sialylation by sialyltransferase involves radiation resistance. *Mol Cancer Res*. 6(8):1316–1325.

Lee M, Lee H-J, Seo WD, Park KH, Lee Y-S. 2010. Sialylation of integrin β1 is involved in radiation-induced adhesion and migration in human colon cancer cells. *Int J Rad Oncol Biol Phys*. 76(5):1528–1536.

Lee M, Park J-J, Ko Y-G, Lee Y-S. 2012. Cleavage of ST6Gal I by radiation-induced BACE1 inhibits golgi-anchored ST6Gal I-mediated sialylation of integrin β1 and migration in colon cancer cells. *Rad Oncol (London, England)*. 7:47–47.

Lee M, Park J-J, Lee Y-S. 2010. Adhesion of ST6Gal I-mediated human colon cancer cells to fibronectin contributes to cell survival by integrin β1-mediated paxillin and AKT activation. *Oncol Rep*. 23:757–761.

Leedham S, Brittan M, McDonald S, Wright N. 2005. Intestinal stem cells. *J Cell Mol Med*. 9(1):11–24.

Leibowitz BJ, Qiu W, Liu H, Cheng T, Zhang L, Yu J. 2011. Uncoupling p53 functions in radiation-induced intestinal damage via PUMA and p21. *Mol Cancer Res*. 9(5):616–625.

Nasirikenari M, Chandrasekaran EV, Matta KL, Segal BH, Bogner PN, Lugade AA, Thanavala Y, Lee JJ, Lau JTY. 2010. Altered eosinophil profile in mice with ST6Gal-1 deficiency: An additional role for ST6Gal-1 generated by the P1 promoter in regulating allergic inflammation. *J Leukoc Biol*. 87(3):457–466.

Nasirikenari M, Lugade AA, Neelamegham S, Gao Z, Moremen KW, Bogner PN, Thanavala Y, Lau JTY. 2019. Recombinant sialyltransferase infusion mitigates infection-driven acute lung inflammation. *Front Immunol*. 10:48–48.

Nasirikenari M, Segal BH, Ostberg JR, Urbasic A, Lau JT. 2006. Altered granulopoietic profile and exaggerated acute neutrophilic inflammation in mice with targeted deficiency in the sialyltransferase ST6Gal I. *Blood*. 108(10):3397–3405.

Petretti T, Schulze B, Schlag PM, Kemmner W. 1999. Altered mRNA expression of glycosyltransferases in human gastric carcinomas. *Biochim Biophys Acta*. 1428(2–3):209–218.

Qiu W, Carson-Walter EB, Liu H, Epperly M, Greenberger JS, Zambetti GP, Zhang L, Yu J. 2008. PUMA regulates intestinal progenitor cell radiosensitivity and gastrointestinal syndrome. *Cell Stem Cell*. 2(6):576–583.

Satyamitra M, Kumar VP, Biswas S, Cary L, Dickson L, Venkataraman S, Ghosh SP. 2017. Impact of abbreviated filgrastim schedule on survival and hematopoietic recovery after irradiation in four mouse strains with different radiosensitivity. *Radiat Res*. 187(6):659–671.

Schultz MJ, Holdbrooks AT, Chakraborty A, Grizzle WE, Landen CN, Buchsbaum DJ, Conner MG, Arend RC, Yoon KJ, Klug CA *et al*. 2016. The tumor-associated glycosyltransferase ST6Gal-I regulates stem cell transcription factors and confers a cancer stem cell phenotype. *Cancer Res*. 76(13):3978–3988.

Singh VK, Newman VL, Berg AN, MacVittie TJ. 2015. Animal models for acute radiation syndrome drug discovery. *Expert Opin Drug Discovery*. 10(5):497–517.

Stoecklein VM, Osuka A, Ishikawa S, Lederer MR, Wanke-Jellinek L, Lederer JA. 2015. Radiation exposure induces Inflammasome pathway activation in immune cells. *J Immunol*. 194(3):1178.

Svensson EC, Soreghan B, Paulson JC. 1990. Organization of the beta-galactoside alpha 2,6-sialyltransferase gene. Evidence for the transcriptional regulation of terminal glycosylation. *J Biol Chem*. 265(34):20863–20868.

Swindall AF, Bellis SL. 2011. Sialylation of the Fas death receptor by ST6Gal-I provides protection against Fas-mediated apoptosis in colon carcinoma cells. *J Biol Chem*. 286(26):22982–22990.

Swindall AF, Londoño-Joshi AI, Schultz MJ, Fineberg N, Buchsbaum DJ, Bellis SL. 2013. ST6Gal-I protein expression is upregulated in human epithelial tumors and correlates with stem cell markers in normal tissues and colon cancer cell lines. *Cancer Res*. 73(7):2368–2378.

Wang PH, Lee WL, Lee YR, Juang CM, Chen YJ, Chao HT, Tsai YC, Yuan CC. 2003. Enhanced expression of alpha 2,6-sialyltransferase ST6Gal I in cervical squamous cell carcinoma. *Gynecol Oncol*. 89(3): 395–401.

Weinstein J, Lee EU, McEntee K, Lai PH, Paulson JC. 1987. Primary structure of beta-galactoside alpha 2,6-sialyltransferase. Conversion of membrane-bound enzyme to soluble forms by cleavage of the NH2-terminal signal anchor. *J Biol Chem*. 262(36):17735–17743.

Wichert B, Milde-Langosch K, Galatenko V, Schmalfeldt B, Oliveira-Ferrer L. 2018. Prognostic role of the sialyltransferase ST6GAL1 in ovarian cancer. *Glycobiology*. 28(11):898–903.

Williams JP, McBride WH. 2011. After the bomb drops: A new look at radiation-induced multiple organ dysfunction syndrome (MODS). *Int J Radiat Biol*. 87(8):851–868.

Yasukawa Z, Sato C, Kitajima K. 2005. Inflammation-dependent changes in α2,3-, α2,6-, and α2,8-sialic acid glycotopes on serum glycoproteins in mice. *Glycobiology*. 15(9):827–837.

Yu J. 2013. Intestinal stem cell injury and protection during cancer therapy. *Transl Cancer Res*. 2(5):384–396.